Chin. Geogra. Sci. 2010 20(5) 461–470
DOI: 10.1007/s11769-010-0420-6

Gold Resources Potential Assessment in Eastern Kunlun Mountains of China Combining Weights-of-evidence Model with GIS Spatial Analysis Technique

HE Binbin[1], CHEN Cuihua[2], LIU Yue[2]

(*1. Institute of Geo-spatial Information Science and Technology, University of Electronic Science and Technology of China, Chengdu 610054, China; 2. College of Geosciences, Chengdu University of Technology, Chengdu 610059, China*)

Abstract: Resources potential assessment is one of the fields in geosciences, which is able to take great advantage of GIS technology as a substitution of traditional working methods. The gold resources potential in the eastern Kunlun Mountains, Qinghai Province, China was assessed by combining weights-of-evidence model with GIS spatial analysis technique. All the data sets used in this paper were derived from an established multi-source geological spatial database, which contains geological, geophysical, geochemical and remote sensing data. Three multi-class variables, i.e., structural intersection, Indosinian k-feldspar granite and regional fault, were used in proximity analysis to examine their spatial association with known gold deposits. A prospectivity map was produced by weights-of-evidence model based on seven binary evidential maps, all of which had passed a conditional independence test. The study area was divided into three target zones of high potential, moderate potential and low potential areas, among which high potential areas and moderate potential areas accounted for 20% of the total area and contained 32 of the 43 gold deposits. The results show that the gold resources potential assessment in the eastern Kunlun Mountains has a higher precision.

Keywords: weights-of-evidence model; mineral resources potential assessment; eastern Kunlun Mountains; spatial analysis; conditional independence

1 Introduction

Resources potential assessment is one of the fields in geosciences, which is able to take great advantage of GIS technology as a substitution of traditional working methods. GIS methods have surpassed the human mind in their capability to integrate and analyze quantitatively large amounts of spatially referenced data (Nykänen and Ojala, 2007). Meanwhile, the application of GIS has great potential for cost savings in mineral resources exploration, because the areas that may endow potential undiscovered deposits can be easily recognized by GIS techniques.

Weights-of-evidence model was originally derived from quantitative medical diagnosis (Aspinall and Hill, 1983; Spiegelhalter and Knill-Jones, 1984); subsequently, it was developed and applied by Bonham Carter *et al*. (1989) and Agterberg *et al*. (1990) for mineral resources quantitative assessment. In recent years, there have been growing literatures on the application of weights-of-evidence model for mineral exploration (Carranza, 2004; Daneshfar *et al*., 2006), and the model has also been applied in other fields such as animal habitats (Romero and Luque, 2006), geologic hazards (Zahiri *et al*., 2006; Neuhäuser and Terhorst, 2007; Song *et al*., 2008), groundwater resources (Cheng, 2004; Corsini *et al*., 2009) and hydrology pollution (Masetti *et al*., 2007). In the last few years, some other spatial statistical models also have been used in mineral resources assessment, such as logistic regression model (Agterberg *et al*., 1993; Sahoo and Pandala, 1999; Carranza and Hale, 2001), fuzzy logic model (Luo and Dimitrakopoulos, 2003), artificial neural networks model (Koike *et al*., 2002; Rigol-Sanchez *et al*., 2003; Nykänen, 2008). Compared

Received date: 2010-01-10; accepted date: 2010-06-22
Foundation item: Under the auspices of National High-tech R&D Program of China (No. 2007AA12Z227), National Natural Science Foundation of China (No. 40701146)
Corresponding author: HE Binbin. E-mail: binbinhe@uestc.edu.cn

with other models, the weights-of-evidence model has some advantages in assessing mineral resources: 1) the weights are relatively easy to be interpreted, they can be confirmed independently, and the favorable targets can be identified easily from the posterior probability or the sum of weights for visual analysis; 2) using proximity analysis to obtain optimal cut-offs, the method provides better estimates for contrast, studentised contrast and buffer size; and 3) it also can be used to capture suitable fuzzy membership (Cheng and Agterberg, 1998; Porwal *et al*., 2003). In addition, missing data could be used in the weights-of-evidence model by mask analysis as well.

In this paper, the gold resources potential in the eastern Kunlun Mountains, Qinghai Province, China is assessed by combining weights-of-evidence model with GIS spatial analysis techniques. The paper involves three main aspects: 1) analyzing the ore-controlled factors from geological, geophysical, geochemical and remote sensing data and then selecting the optimal ore-controlled variables; 2) testing conditional independence of evidence maps; and 3) integrating evidence maps and making the ultimate potential map of gold deposits based on the posterior probability. This paper will be helpful for better understanding the ore-controlled factors and future explorating undiscovered gold deposits in the eastern Kunlun Mountains, China.

2 Geologic Setting of Study Area

The eastern Kunlun Mountains orogenic belt, located in Qinghai Province, Northwest China, is attached to the southern margin of the Qaidam Massif (Wang *et al*., 1990; Qian *et al*., 2000) and the north margin of the North Bayan Har orogenic belt (Fig. 1). The study area is characterized by three major deep crustal-scale faults of the northern Kunlun fault, central Kunlun fault and southern Kunlun fault (Jiang *et al*., 1992; Xu *et al*., 1996). According to the volcanic assemblages, sedimentation formation and mineralization, the eastern Kunlun orogenic belt can be divided into the northern Kunlun Qimantage back-arc basin, the central Kunlun basement uplift and granitic belt and the southern Kunlun composite belt (Pan *et al*., 2006) (Fig. 2). The eastern Kunlun Mountains has undergone multi-cyclic composite orogenic processes with a complex evolutionary history (Pan *et al*., 1996; Yin and Zhang, 1997), mainly involving four tectonic cycles (Li *et al*., 2007): pre-Cambrian palaeocontinent formation (orogenic basement), Caledonian orogenic cycle, late Variscan-Indosinian orogenic cycle, and Mesozoic-Cenozoic orogenic cycle, of which the Variscan-Indosinian orogenic movement is closely associated with metal mineralization (Xu *et al*., 2001; Feng *et al*., 2004).

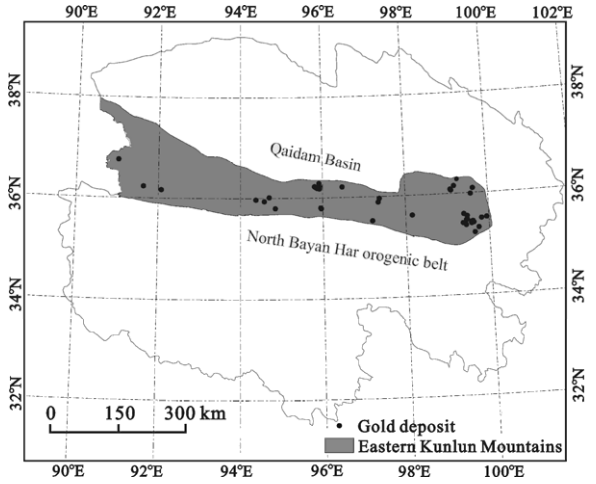

Fig. 1 Location of eastern Kunlun Mountains in Qinghai Province of China and gold deposits

The exposed major stratigraphic and lithologic units underlying the study area are displayed in Fig. 2. The Elashan Formation of the Triassic consists of basic and intermediate-acid volcanic rocks with sandstone intercalations. The Nachitai Group of the Ordovician consists largely of schist, mafic volcanic rocks, chert and crystalline limestone. The Jinshuikou Group, which is the oldest crystalline basement that comprises gneiss, amphibolite rocks, migmatite and marble, belongs to a suite of middle-high grade metamorphic rocks (Wang *et al*., 2004). The Maoniushan Formation of the Devonian is composed of an upper unit of basic and intermediate-acid volcanic rocks underlain by clastic rocks. The Tanjianshan Group of the Ordovician-Cambrian is composed of intermediate-mafic volcanic rocks, phyllite crystalline limestone and sandstone. The Wanbaogou Group of Sinian-Cambrian is subdivided into an upper unit and a lower unit: the upper unit, comprising carbonate rock, is mainly marble and dolomite, which belongs to the pre-Cambrian fold basement with low-grade metamorphism; the lower unit is composed of intermediate-mafic volcanic rock belonging to Sinian (Pan *et al*., 1996). Volcanic rock and carbonaceous sl-

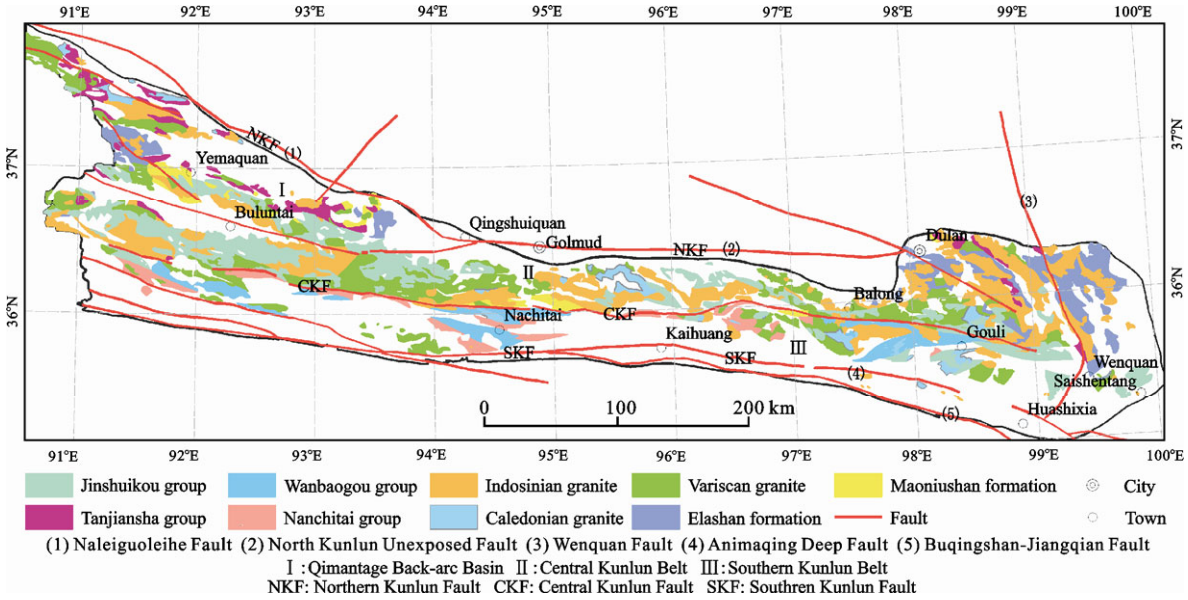

Fig. 2 Simplified geological map of eastern Kunlun Mountains of Qinghai Province

ate of the Wanbaogou Group serve as important source beds of precious metal (Au) and non-ferrous metals (e.g., Cu, Co, Ni, *etc*.) in the southern Kunlun composite belt (Guo *et al*., 2004). In the study area, exposed magmatic rocks are mainly composed of granites of various periods, of which Variscan-Indosinian granite is closely associated with the metalliferous mineralization in the regional scale, when it occurs extensively, diversely and permanently in a metallogenic environment (Qian *et al*., 2000).

3 Materials and Methods

3.1 Data sources

All the data sets were derived from a multi-source geospatial database (MGSDB) established by Institute of Geo-spatial Information Science and Technology, University of Electronic Science and Technology of China in 2009, which contains geological, geophysical, geochemical and remote sensing data. The data sets were processed with ArcView Spatial Analyst ESRI software and a plug-in extension for multi-criteria approaches, Arc-SDM (Kemp *et al*., 1999).

3.2 Weights-of-evidence model

Weights-of-evidence (WofE) model is based on Bayesian conditional probability to determine the optimum binary pattern of a geological feature that shows spatial association with a set of mineral deposits (Bonham-Carter *et al*., 1989; Agterberg *et al*., 1990). After quantifying the spatial association, binary predictor patterns can be created and used as inputs to the predictive models. The output predictive maps indicate the probability of deposits and the uncertainties associated with them.

Suppose that the *j*th binary map is B_j and D refers to the presence of deposits, the positive weight of evidence (W^+) is defined as (Bonham-Carter *et al*., 1989; Agterberg *et al*., 1990):

$$W^+ = \log_e \frac{P(B_j/D)}{P(B_j/D')} \tag{1}$$

and the negative weight of evidence (W^-) is defined as (Bonham-Carter *et al*., 1989; Agterberg *et al*., 1990):

$$W^- = \log_e \frac{P(B_j'/D)}{P(B_j'/D')} \tag{2}$$

where $P(B_j/D)$ is the conditional probability of the presence of the *j*th binary map, giving the presence of a deposit; $P(B_j/D')$ is the conditional probability of the presence of the *j*th binary map, giving the absence of a deposit; $P(B_j'/D)$ is the conditional probability of the absence of the *j*th binary map , giving the presence of a deposit; $P(B_j'/D')$ is the conditional probability of the absence of the *j*th binary map, giving the absence of a deposit.

The contrast C_j for the *j*th map is an overall measure of spatial association between the deposits and the binary pattern (Bonham-Carter *et al*., 1989; Agterberg *et al*., 1990):

$$C_j = W_j^+ - W_j^- \quad (3)$$

And, the variance of the weights, $s(C_j)$, for the jth map is defined as (Bonham-Carter *et al*., 1989; Agterberg *et al*., 1990):

$$s(C_j) = \sqrt{s^2(W_j^+) - s^2(W_j^-)} \quad (4)$$

$C_j > 0$ if the spatial association is positive, $C_j < 0$ if the spatial association is negative, and $C_j = 0$ if there is no spatial association. Sometimes, C_j, particularly with a small number of deposits, has no significant larger value and no significance (Carranza, 2004); however, studentised contrast, $Stud(C_j)$, as the ratio of contrast to its standard deviation, $C_j / s(C_j)$, provides a more reliable measure of spatial correlation (Bonham-Carter, 1994; Porwal *et al*., 2001). In this paper, the optimal thresholds are derived from multi-class evidential maps based on the $Stud(C_j)$ value when using proximity analysis in weights-of-evidence model.

The conditional independence (CI) test is critical to weights-of-evidence model, since its violation will result in the posterior probability either being over or underestimated. Generally, three conditional independence tests were used to determine whether the assumption of conditional indepedence was satisfied: 1) chi-square test; 2) Kolmogorov-Smirnov test; and 3) overall test (OT), which was employed to compare observed deposits and expected deposits, and can be calculated as follows (Bonham-Carter, 1994):

$$OT = \frac{N(D)}{N(D)_{\text{pred}}} \quad (5)$$

$$N(D)_{\text{pred}} = \sum_{k=1}^{m} P_k N(A)_k \quad (6)$$

where $N(D)$ represents the observed number of deposits, and $N(D)_{\text{pred}}$ represents the expected number of deposits, P_k is the probability of the kth unique condition, $N(A)_k$ represents the number of the deposits in the kth unique condition.

3.3 Selection of ore-controlled factors

3.3.1 Structural factors

To investigate further the relationship between known deposits and various scales of structural information at a regional scale is an important way to understand the mineralization and distribution of hydrothermal deposits. Structural intersections usually provide structural favorability for magmatism that can increase the probability of large deposits appearing. Furthermore, structural intersections are special positions that represent the distribution of tectonic stress, and the extent of rock-damage by intense trans-pressional or trans-tensional tectonic strain may serve as conduits for magma ascent to the shallow crust. Pooling of large volumes of deeply derived magma in shallow crustal magma chambers may then lead to the formation of hydrothermal mineral deposits (Chernicoff *et al*., 2002). Using image processing/analysis techniques, the lineaments were extracted from remote sensing data, and then structural intersections were obtained from the lineaments aided by GIS techniques.

3.3.2 Intrusive rock

The study area was subjected to multi-stage magmatism, especially, during the Variscan and Indosinian periods, when extensive region-wide intrusion of acid magma occurred, which led to ore-formation in favorable pressure-reduced areas and also controlled the distribution of gold deposits to some degree.

3.3.3 Mineral alteration

LandSat data have been used for a number of years in arid and semi-arid environments to locate areas of iron oxides and/or hydrous minerals, especially for areas covered by sparse vegetation. Generally, shallow chemical weathering areas are more favorable for the use of optical remote sensing techniques for alteration mapping. Our analysis focuses on the spatial distribution of the main types of hydrothermally altered rocks as a means of determining the general extent of potential Au-mineralization. Enhanced Thematic Mapper plus (ETM^+) images were used in the study area for extracting altered minerals.

3.3.4 Other ore-controlled factors

After detailed studying for the metallogenic features of the gold deposits in the eastern Kunlun Mountains, other three ore-controlled factors were also selected, gold anomaly, Tugen Formation and Elashan Formation. They were used as binary evidential maps for integrating in weights-of-evidence model.

4 Results

4.1 Spatial analysis of ore-controlled factors

4.1.1 Structural factors

Structural intersections were buffered with 500 m wide buffer bands (Fig. 3a). The maximum studentised contrast occurred at the distance of 4 000 m, indicating that

there existed highest spatial association with the known deposits in this range. Within the range of 4 000 m, there were 15 of the 43 gold deposits, covering 35% of the total gold deposits, which was selected as a binary map pattern for the following analysis (Fig. 4).

Using proximate analysis, successive corridors were created around regional faults. The optimal threshold, calculated by finding the highest *Stud*(*C*) value, occurred at a distance of 1 500 m (Fig. 3b), and 11 of 43 gold deposits were distributed in the range of 1 500 m, covering 26% of the total gold deposits. The distance inside 1 500 m was selected as a binary pattern and applied in mapping mineral potential (Fig. 4).

4.1.2 Intrusive rocks

Contrast and studentised contrast were calculated for each cumulative buffer band. The highest *Stud*(*C*) value occurred at the distance of 4 000 m (Fig. 3c), and this pattern contained 11 of 43 deposits, covering 6% of the total area and contained 26% of the total gold deposits. Most of the calculated *C* values were greater than 1 and the *Stud*(*C*) values were greater than 3, which were obviously higher than the corresponding values derived from regional faults and structural intersections. The results indicate that Indosinian k-feldspar granites have a better spatial association with gold deposits respect to regional faults and structural intersections. The distance inside 1 500 m was selected as a binary pattern and applied in mapping mineral potential (Fig. 5).

4.1.3 Mineral alteration

Since the Proterozoic, the Eastern Kunlun Mountains has suffered a wide range of magmatic hydrothermal intrusive activities and multi-stage structural movements, wh-

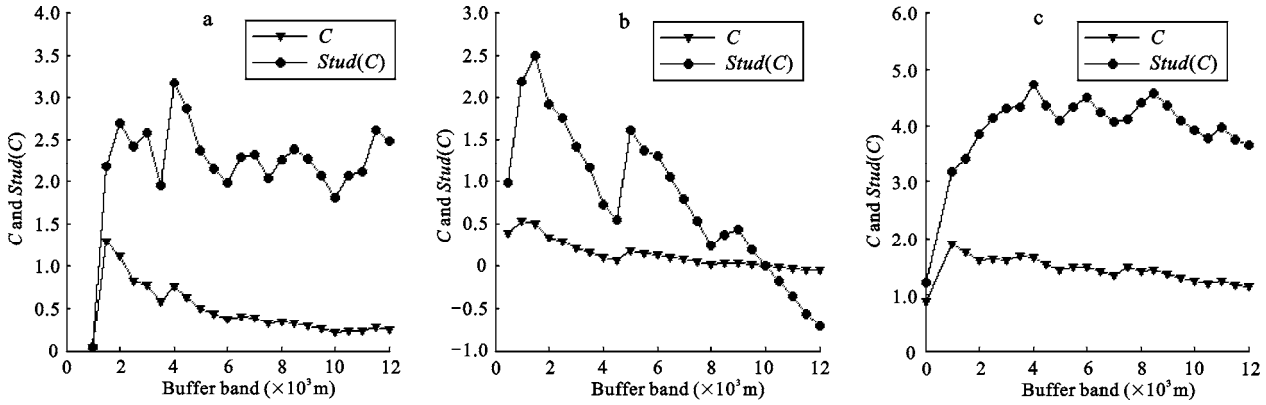

(a) structural intersection; (b) regional fault; (c) Indosinian k-feldspar granite

Fig. 3 Relationships between different ore-controlling components and buffer widths

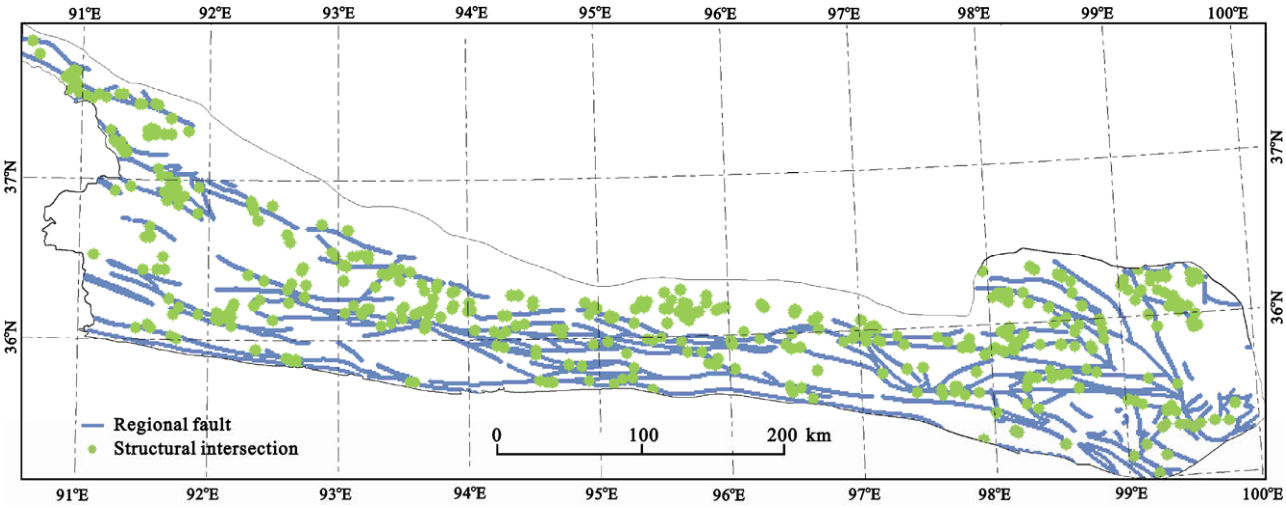

Structural intersections were interpreted within 4000 m buffer band, regional faults were interpreted within 1500 m buffer band

Fig. 4 Binary map parrens used to predict gold deposits based on proximite analysis

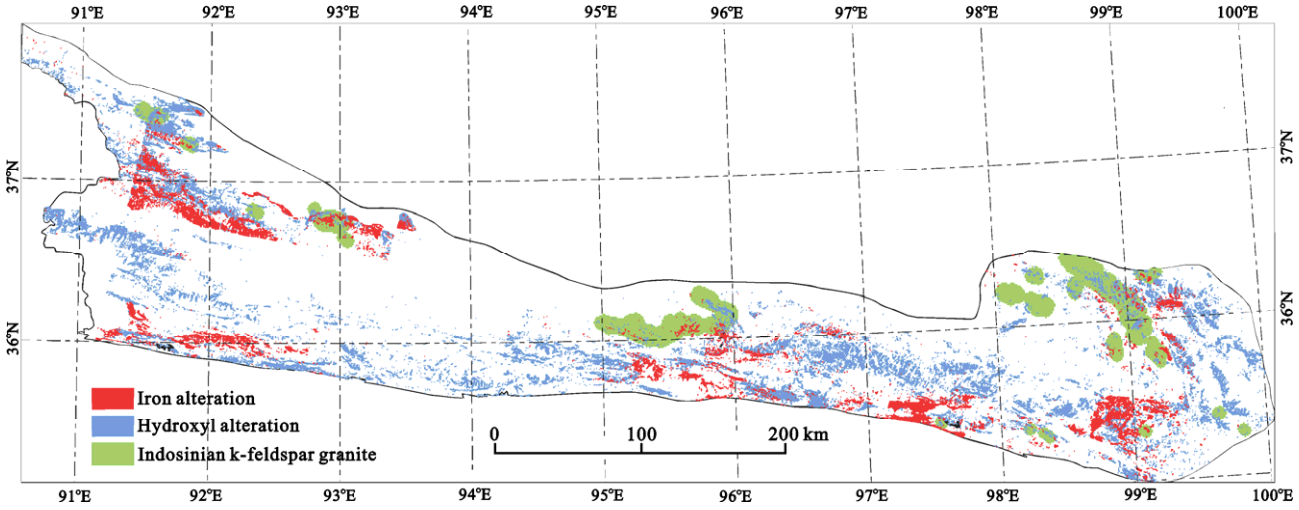

Fig. 5 Altered mineral information interpreted from ETM$^+$ and Indosinian k-feldspar granite within 4000 m buffer band

ich led to extensive hydrothermal alteration and the exposure of large areas of basement. In addition, the study area located in the western China is arid or semi-arid, with sparsely vegetated regions. All of these are advantages for the use of remote sensing technology for macro-monitoring. In this paper, using principal component analysis, iron oxides and hydroxyl-bearing minerals were extracted from ETM$^+$ data (Fig. 5). Spatial analysis aided by the weights-of-evidence method indicates that hydroxyl alteration has a higher spatial association with known gold deposits than iron oxides alteration.

4.2 Conditional independence test

4.2.1 Chi-square test

A pair-wise conditional independence test was carried out on the three multi-class and four binary evidential maps (Table 1). The results indicate that the assumption of conditional independence is not violated at the 0.05 significance level with one degree of freedom based on the x^2 test.

4.2.2 Kolmogorov-Smirnov test

The goodness-of-fit between the observed frequencies of gold deposits and the expected frequencies based on the calculated posterior probabilities was tested using the Kolmogorov-Smirnov test (Fig. 6). The maximum difference between obseved gold deposits and expected gold deposits is 0.1222, which is lower than 0.1403 at the 0.05 significance level with 94 degrees of freedom based on the Kolmogorov-Smirnov test. The result indicates that the null hypothesis can be accepted at the 95% confidence level.

4.2.3 Overall test

Bonham-Carter (1994) suggested that if $OT > 0.85$, based on empirical considerations, then assumption of CI is not violated seriously; otherwise, assumption of CI is violated seriously. In this paper, the number of observed gold deposits is 43, and the number of expected gold deposits calculated from $N(D)_{\text{pred}}$ is 50.2, and $OT \approx 0.86$, which indicates that the correlations among geological variables are not significant.

4.3 Posterior probability map

The predictive map is a synthesis of the spatial association rules established and quantified during the preceding

Table 1 Calculated x^2 values for testing conditional independence between all pairs of binary maps

Binary predictor map	Gold anomaly	Structural intersection	Elashan Formation	Tugen Formation	k-feldspar granite	Hydroxyl alteration
Regional fault	0.45	0.06	1.04	0.08	0.92	0.01
Gold anomaly		0.00	0.17	0.29	2.58	0.06
Structural intersection			0.01	0.19	1.49	0.95
Elashan Formation				0.01	0.22	2.27
Tugen Formation					0.40	0.14
k-feldspar granite						0.07

Note: Tabulated x^2 value at 0.05 significance level for one degree of freedom is 3.84

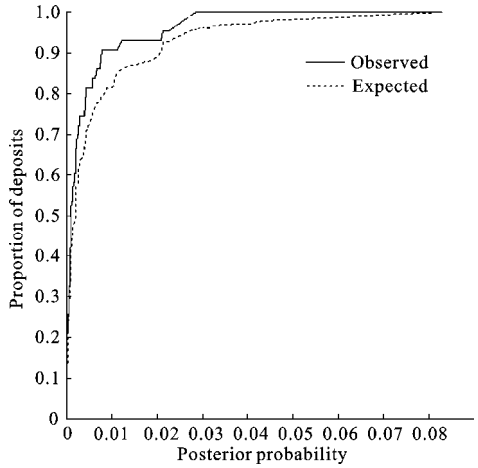

Fig. 6 Variation of cumulative expected and observed frequencies of gold deposits with posterior probability

stages. Its objective is to produce a picture of the gold potential of the study area in order to 1) reach a better understanding of the factors controlling the distribution of the mineralization, and 2) trigger eventual exploration work in new areas. For the latter reason, it is also called a prospectivity map. The prospectivity map provides a better understanding of areas where minerals have been found in the past, and mineral deposits may occur in the future exploration.

Generally, posterior probabilities derived from weights-of-evidence model are used for mineral potential mapping. As shown in Fig. 7a, the posterior probability slowly increases initially and rapidly increases later with the percentage of the cumulative area. The same variation trend can also be seen in Fig. 7b, which shows the variations of cumulative deposits with cumulative area. Two inflection points can be identified in each curve (Fig. 7), at which the slope of the curve changes from approximately flat to moderate and from moderate to steep. Thus, three target zones can be identified from the two inflection points. We define the three target zones as high potential area, moderate potential area and low potential area, respectively.

The threshold probability corresponding to the lower and the upper inflection points on the curve in Fig. 7a are 0.0005 and 0.0011, respectively. The threshold probabilities corresponding to the lower and the upper inflection points on the curve in Fig. 7b are 11 and 21, respectively. Low potential areas contain 25.6% (11 deposites) of the total gold deposits, covering 80% of the total area; the high potential areas contain 48.8% (21 deposits) of the total gold deposits, covering 9% of the total area; and the moderate potential areas contain 25.6% (11 deposits) of the gold deposits, covering 11% of the total area (Fig. 7b).

Figure 8 shows the gold deposits potential based on weights-of-evidence model. Obviously, high potential areas are distributed in three places in the eastern Kunlun Mountains, which objectively reflect the spatial distribution of known deposits and the extension of the regional deep-seated faults, spatially expressing E-W and N-W trending extensions. Several higher potential (high and moderate potential) areas can be identified from the prospectivity map, such as Yemaquan District (36°50′–37°40′N and 91°00′–92°00′E) near the Central Kunlun Fault and Dulan district (36°00′–36°20′N and 98°00′–99°00′E) in the eastern part of the study area. Though there are no discovered deposits, those areas should be taken into account for the future mineral exploration.

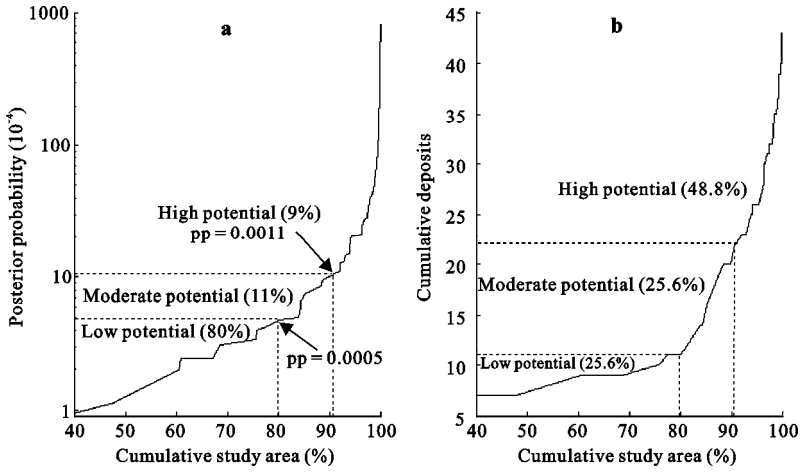

Fig. 7 Variations of posterior probability (pp) (a) and cumulative gold deposits (b) with cumulative percent of study area

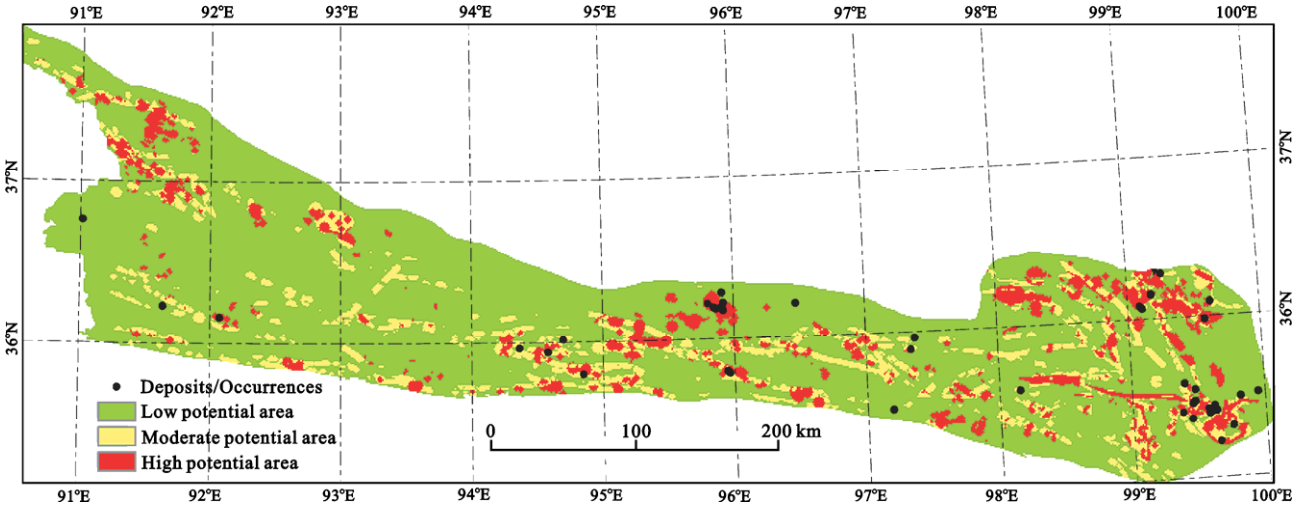

Fig. 8 Gold deposits potential map in eastern Kunlun Mountains

5 Conclusions

Integration of multi-source geology spatial data sets into a single reference system enables a better understanding of the parameters controlling a region′s metallogeny, in terms of both space and time. Favorable potential areas identified in the study area were obviously restricted by regional deep-seated faults, especially, the three crustal-scale faults (Fig. 2).

In order to account for complex spatial patterns of multi-source geology spatial data sets in geological thematic mapping, a GIS-based spatial analysis technique was presented and applied to mineral resources assessment. For an example, using proximity analysis and statistical analysis to investigate spatial association between geological variables and mineral deposits based on weights-of-evidence model.

Conditional independence test was performed using three different methods to measure the degree of spatial association between evidential maps and gold deposits. All the binary maps selected passed the conditional independence test.

Posterior probability map calculated from seven binary evidential maps produced a better prediction rate. Twenty percentage of the area predicted was considered as higher potential (high and moderate potential) areas which contained 32 of 43 gold deposits, of which high potential area occupied 9% of the total area, and contained 48.8% of the total gold deposits. The method discussed in this paper is a decision-making process from the point of view of GIS with additional quantitative evidence. The prediction results can be considered as important reference information for future mineral assessments because of their objective nature and strict application of the procedures of weights-of-evidence analysis.

Acknowledgement

We express our gratitude to Zhuang Yongcheng from Qinghai Institute of Geology Survey for his directions and advices.

References

Agterberg F P, Bonham-Carter G F, Cheng Q *et al*., 1993. Weights of evidence model and weighted logistic regression in mineral potential mapping. In: Davis J C *et al*. (eds.). *Computers in Geology*. New York: Oxford University Press, 13–32.

Agterberg F P, Bonham-Carter G F, Wright D F, 1990. Statistical pattern integration for mineral exploration. In: Gaál G *et al*. (eds.). *Computer Applications in Resource Estimation Prediction and Assessment for Metals and Petroleum*. Oxford-New York: Merriam Pergamon Press, 1–21.

Agterberg F P, Cheng Q, 2002. Conditional independence test for weights-of-evidence model. *Natural Resources Research*, 11(4): 249–255. DOI: 10.1023/A:1021193827501

Aspinall P J, Hill A R, 1983. Clinical inferences and decisions—I. Diagnosis and Bayes′ theorem. *Ophthalmic and Physiologic Optics*, 3: 295–304.

Bonham-Carter G F, 1994. *Geographic Systems for Geoscientists: Modeling with GIS*. Oxford: Pergamon Press.

Bonham-Carter G F, Agterberg F P, Wright D F, 1989. Weights of evidence modelling: A new approach to mapping mineral potential. In: Agterberg F P *et al*. (eds.). *Statistical Applica-*

tions in the Earth Sciences. Geology Survey of Canada, Paper 89–9: 171–183.

Carranza E J M, 2004. Weights of evidence model of mineral potential: A case study using small number of prospects, Abra, Philippines. *Natural Resources Research*, 13(3): 173–187. DOI: 10.1023/B:NARR.0000046919.87758.f5

Carranza E J M, Hale M, 2001. Logistic regression for geologically constrained mapping of gold potential, Baguio District, Philippines. *Exploration and Mining Geology*, 10(3): 165–175. DOI: 10.2113/0100165

Cheng Q, 2004. Application of weights of evidence method for assessment of flowing wells in the Greater Toronto area, Canada. *Natural Resources Research*, 13(2): 77–86. DOI: 10.1023/B:NARR.0000032645.46747.48

Cheng Q, Agterberg F P, 1998. Fuzzy weights of evidence method and its applications in mineral potential mapping. *Natural Resource Research*, 8(1): 27–35. DOI: 10.1023/A:102167751064-9

Chernicoff C J, Richards J P, Zappettini E O, 2002. Crustal lineament control on magmatism and mineralization in northwestern Argentina: Geological, geophysical, and remote sensing evidence. *Ore Geology Reviews*, 21: 127–155. DOI: 10.10-16/S0169-1368(02) 00087-2

Corsini A, Cervi F, Ronchetti F, 2009. Weight of evidence and artificial neural networks for potential groundwater spring mapping: An application to the Mt. Modino area (Northern Apennines, Italy). *Geomorphology*, 111: 79–87. DOI: 10.1016/j.geomorph.2008.03.015

Daneshfar B, Desrochers A, Budkewitsch P, 2006. Mineral-potential mapping for MVT deposits with limited data sets using Landsat data and geological evidence in the Borden basin, northern Baffin island, Nunavut, Canada. *Natural Resources Research*, 15(3): 129–149. DOI: 10.1007/s11053-006-9020-7

Feng Chengyou, Zhang Dequan, Wang Fuchun *et al*., 2004. Geochemical chracteristics of ore-forming fluids from the orogenic Au (and Sb) deposits in the East Kunlun area, Qinghai Province. *Acta Petrologica Sinica*, 20(4): 949–960. (in Chinese)

Guo Xiaodong, Zhang Yujie, Liu Guige *et al*., 2004. Metallogenic regularities and prospecting direction of gold and copper in eastern Kunlun. *Gold Geology*, 10(4): 16–22. (in Chinese)

Jiang Chunfa, Yang Jingsui, Feng Binggui, 1992. *Opening closing tectonics of Kunlun Mountains*. Beijing: Geological Publishing House, 1–224. (in Chinese)

Kemp L D, Bonham-Carter G F, Raines G L, 1999. Arc-WofE: ArcView extension for weights of evidence. http://gis.nrcan.gc.ca/software/arcview/ wofe.

Koike K, Matsuda S, Suzuki T *et al*., 2002. Neural network-based estimation of principal metal contents in the Hokuroku District, northern Japan, for exploring Kuroko-type deposits. *Natural Resources Research,* 11(2): 135–156. DOI: 10.1023/A:1015520204066

Li Zhiming, Xun Chunji, Wang Xiaohu *et al*., 2007. Features of regional mineralization and analysis of the exploration development in the eastern Kunlun Mountains. *Geological Review*, 53(5): 708–718. (in Chinese)

Luo X, Dimitrakopoulos R, 2003. Data-driven fuzzy analysis in quantitative mineral resource assessment. *Computers & Geosciences,* 29(1): 3–13. DOI: 10.1016/S0098-3004(02)00078X

Masetti M, Poli S, Sterlacchini S, 2007. The use of the weights-of-evidence model technique to estimate the vulnerability of groundwater to nitrate contamination. *Natural Resources Research*, 16(2): 109–119. DOI: 10.1007/s11053-0079045-6

Neuhäuser B, Terhorst B, 2007. Landslide susceptibility assessment using ″weights-of-evidence″ applied to a study area at the Jurassic escarpment (SW-Germany). *Geomorphology*, 86: 12–24. DOI: 10.1016/j.geomorph.2006.08.002

Nykänen V, 2008. Radial basis functional link nets used as a prospectivity mapping tool for orogenic gold deposits within the central Lapland Greenstone Belt, Northern Fenno- scandian Shield. *Natural Resources Research*, 17(1): 29–48. DOI: 10.1007/s11053-008-9062-0

Nykänen V, Ojala V J, 2007. Spatial analysis techniques as successful mineral-potential mapping tools for orogenic gold deposits in the northern Fennoscandian Shield, Finland. *Natural Resources Research*, 16(2): 85–92. DOI: 10.1007/s11053-007-9046-5

Pan Tong, Luo Cairang, Yi Youchang *et al*., 2006. *Metallogenic Regularity and Metallogenic Prognosis of Metal Ores in Qinghai Province*. Beijing: Geological Publishing House. (in Chinese)

Pan Yusheng, Zhou Weiming, Xu Ronghua *et al*., 1996. The early Palaozoic geological features and evolutions of the Kunlun mountain. *Science in China* (*Series D*), 26(4): 302–307. (in Chinese)

Porwal A, Carranza E J M, Hale M, 2001. Extended weights-of-evidence model for predictive mapping of base metal deposit potential in Aravalli Province, western India. *Exploration and Mining Geology*, 10(4): 273–287. DOI: 10.2113/0100273

Porwal A, Carranza E J M, Hale M, 2003. Knowledge-driven and data-driven fuzzy Models for predictive mineral potential mapping. *Natural Resources Research*, 12(1): 1–25. DOI: 10.1023/A:1022693220894

Qian Zhuangzhi, Huzhengguo, Liu Jiqing *et al*., 2000. Active continental margin and regional metallogenesis of the palaeotethys in the Eastern Kunlun Mountains. *Geotectonica et Metallogenia*, 24(2): 134–139. (in Chinese)

Rigol-Sanchez J P, Chica-Olmo M, Abarca-Hernandez F, 2003. Artificial neural networks as a tool for mineral potential mapping with GIS. *International Journal of Remote Sensing,* 24(5): 1151–1156. DOI: 10.1080/0143116021000031791

Romero C R, Luque S, 2006. Habitat quality assessment using Weights-of-Evidence based GIS model: The case of Picoides tridactylus as species indicator of the biodiversity value of the Finnish forest. *Ecological Model*, 196: 62–76. DOI: 10.1016/j.ecolmodel.2006.02.017

Sahoo N R, Pandala H S, 1999. Integration of Sparse Geologic Information in Gold Targeting Using Logistic Regression Analysis in the Hutti-Maski Schist Belt, Raichur, Karnataka, India—A Case Study. *Natural Resources Research*, 8(3): 233–

250. DOI: 10.1023/A:1021698115192

Spiegelhalter D J, Knill-Jones R P, 1984. Statistical and knowledge-based approaches clinical decision support systems, with an application in gastroenterology. *Journal of the Royal Statistical Society*, 1: 35–77.

Song R, Hiromu D, Kazutoki A *et al.*, 2008. Model the potential distribution of shallow-seated landslides using the weights of evidence method and a logistic regression model: A case study of the Sabae Area, Japan. *International Journal of Sediment Research*, 23: 106–118. DOI: 10.1016/S1001-6279(08)60010-4

Wang Guocan, Wang Qinghai, Jian Ping *et al*., 2004. Zircon SHRIMP ages of precambrian metamorphic basement rocks and their tectonic significance in the eastern Kunlun mountains, Qinghai Province, China. *Earth Science Frontiers*, 11(4): 481–490. (in Chinese)

Wang Hongzhen, Yang Sennan, Liu Benpei *et al.*, 1990. *The Tectono-palaeogeography and Biogeography of China and Adjacent Regions in the Carboniferous Period*. Wuhan: China University of Geosciences Press, 1–17. (in Chinese)

Xu Wenyi, Zhang Dequan, Yan Shenghao *et al.*, 2001. Achievements and prospecting of the mineral resources survey in eastern Kunlun area. *Chinese Geology*, 28(1): 25–29. (in Chinese)

Xu Zhiqin, Jiang Mei, Yang Jingsui, 1996. Tectonophysical process at depth for the uplift of the northern part of the Qinghai-Tibet plateau: Illustrated by the geological and geophysical conprehensive profile from Golmud to the Tanggula Mountains, Qinghai Province, China. *Acta Geologica Sinica*, 70(3): 195–206. (in Chinese)

Yin Hongfu, Zhang Kexin, 1997. Characteristics of the Eastern Kunlun orogenic belt. *Earth Science—Journal of China University of Geoscience*, 22(4): 339–342. (in Chinese)

Zahiri H, Palamara D R, Flentje P *et al*., 2006. A GIS-based weights-of-evidence model for mapping cliff instabilities associated with mine subsidence. *Environmental Geology*, 51: 377–386. DOI: 10.1007/s00254-006-0333-y